Supporting Information

Dual functional Cyclometalated Iridium Imine NHC Complexes: Highly Potent Anticancer and Antimetastatic Agents

Zhenzhen Tian [a‡], Yuliang Yang [a‡], Lihua Guo [a], Genshen Zhong [b], Juanjuan Li [a], Zhe Liu[a*]

[a] Institute of Anticancer Agents Development and Theranostic Application, The Key Laboratory of Life-Organic Analysis and Key Laboratory of Pharmaceutical Intermediates and Analysis of Natural Medicine, Department of Chemistry and Chemical Engineering, Qufu Normal University, Qufu 273165, China.

[b] Henan Collaborative Innovation Center of Molecular Diagnosis and Laboratory Medicine, School of Laboratory Medicine, Xinxiang Medical University, Xinxiang 453003, China.

‡The first two authors are equal first authors.

*Corresponding author. Email: liuzheqd@163.com

Supporting Information

Experimental Section

Materials

All reagents were used as received, unless noted otherwise. $IrCl_3 \cdot nH_2O$, 1-methylimidazole, 1-ethylimidazole, 1-isopropylimidazole, acetyl chloride, 2,6-dimethylaniline, 2,6-diisopropylaniline, 1-phenylpyrazole (ppz) and triphosgene were purchased from Sigma-Aldrich and used without further purification unless otherwise specified. Tetrahydrofuran were refluxed over metallic sodium for 24 h before being used. Dichloromethane were dried over phosphorus pentoxide for 8 h before being used. For the biological experiments, CT DNA, DMEM medium, fetal bovine serum, penicillin/streptomycin mixture, trypsin/EDTA, cisplatin, MTT, and phosphate-buffered saline (PBS) were purchased from Sangon Biotech. CCCP (Sigma Aldrich, USA), chloroquine (Sigma Aldrich, USA), EB (Sigma Aldrich, USA) and AO (Sigma Aldrich, USA) were used as received. Testing compounds was dissolved in DMSO and diluted with the tissue culture medium before use. Stock solutions of cisplatin (10 mM) and complexes **Ir1–Ir6** (10 mM) were prepared in DMSO. All stock solutions were stored at -20 °C, thawed and diluted with culture medium prior to each experiment.

Physical Measurements

^1H NMR spectra were acquired in 5 mm NMR tubes at ambient temperature on Bruker DPX 500 spectrometers using TMS as an internal standard and $CDCl_3$ or DMSO as solvent. Mass spectra of the complexes **Ir1-Ir6** were recorded on a Atouflex Speed MALDI-TOF MS. Elemental analysis (C, H, and N) was carried out using a Carlo Erba model EA 1108 microanalyzer. The reported m/z values represent the major peaks with isotopic distribution. X-ray Diffraction data were collected at 298(2) K on a Bruker Smart CCD area detector with graphite-monochromated Mo Kα radiation (λ = 0.71073 Å). UV−Vis spectra were recorded on a TU-1901 UV-Vis recording spectrophotometer.

Crystal structure analysis

Single crystals of complex **Ir4** were obtained. All diffraction data were obtained on a Bruker Smart Apex CCD diffractometer equipped with graphite-monochro mated Mo Kα radiation. Absorption corrections were applied using SADABS program. X-ray Diffraction data were collected at 298(2) K on a Bruker Smart CCD area detector with graphite-monochromated Mo Kα radiation (λ = 0.71073 Å). The structures were solved by direct methods using SHELXS (TREF) with additional light atoms found by Fourier methods. Complexes were refined against F^2 using SHELXL, and hydrogen atoms were added at calculated positions and refined riding on their parent atoms. X-ray crystallographic data for complex **Ir4** are available as **Figure 1**, **Tables S1** and **S2** have been deposited in the Cambridge Crystallographic Data Centre under the accession numbers CCDC 1863514. X-ray crystallographic data in CIF format are available from the Cambridge Crystallographic Data Centre.

Cell lines and Cell culture

The human cervix carcinoma cell lines HeLa, the hepatocellular carcinoma cell lines HepG2,

human lung cancer cell lines A549, mouse glioma cell lines GL261, cisplatin-resistant cell lines A549R and human bronchial epithelial normal cells 16HBE and BEAS-2B were obtained from Shanghai Institute of Biochemistry and Cell Biology (SIBCB). Cells were maintained in DMEM (high glucose, Gibco) media supplemented with fetal bovine serum (10%), 1 % penicillin-streptomycin solution at 37 °C in a CO_2 incubator (5% CO_2).

Cell viability assay and IC_{50} value determination

The cell viability assay was performed by MTT assay. Briefly, cells cultured in 96-well plates were incubated with a series of concentrations of the Ir(III) complexes for 24 h. Then, 15 μL of an MTT solution (5 mg mL^{-1}) was added to each well for 4 h. The liquid was disposed of and 100 μL DMSO was added, the plate was shaken for 5 min and the absorbance intensity at 570 nm was determined by microplate reader (DNM-9606, Perlong Medical, Beijing, China). Similarly, IC_{50} values were calculated by cell viabilities under different incubation concentrations.

Stability in human plasma

The stability of complex **Ir6** in plasma was assessed by using a procedure analogous to a reported method.[1] An diazepam (Sigma-Aldrich) solution was used as internal reference. Complex **Ir6** (20 μM) and 10 μM diazepam and DMSO were added to plasma (975 μL) to a total volume of 1000 μL. The solution was incubated for 0 h or 72 h at 37 °C with shaking (~300 rpm) respectively. The reaction was stopped by adding 2 mL of methanol, and the mixture was centrifuged for 45 min at 1000g at 4 °C. The methanolic was evaporated, and the residue was suspended in 200 μL of 1:1 acetonitrile/H_2O (v/v). The suspension was filtered and analyzed by HPLC-UV. A C18 reverse phase column was used with a flow rate of 0.5 mL/min. The runs were performed with a linear gradient of A (acetonitrile, Sigma-Aldrich HPLC grade) in B (distilled water containing 0.1% HCOOH).

Cellular uptake

A549 cells were seeded in 90 mm dishes for 24 h (three dishes were prepared per compound tested). The media was removed and replaced with fresh media containing the tested **Ir6** (10 μM) for 1 h. After the removal of the culture media and rinse with 3 mL of PBS buffer (1X), the cells were treated with 2 ml of 0.25% trypsin and centrifuged at 1000 rpm. The cells were counted, one half of the cells were centrifuged, quickly washed with PBS, and stored at 253 K for determination of total cell accumulation of iridium. Another half of the samples was used for membrane, nucleus, cytosol and cytoskeleton, using a Subcellular Protein Fractionation Kit for Cultured Cells extraction kit (Thermo Scientific). The samples were nitrolysis with concentrated HNO_3 at 95 ℃ for 2 h, H_2O_2 at 95 ℃ for 1.5 h and concentrated HCl at 37 ℃ for 0.5 h. Finally, the solution was diluted to 2 mL with MQ water and the Ir content was measured by the inductively coupled plasma mass spectrometer (ICP-MS; VG Elemental).

Cell Uptake Mechanism

A549 cells were seeded in 35 mm dishes for 24 h and at 4 ℃ or preincubated with CCCP (10 μM) or chloroquine (50 μM) for 1 h. The medium was removed and the cells were then incubated with **Ir6** (10 μM) for 15 min. Cells were collected and rinsed, and the extent of uptake was analyzed by ICP-MS.

Cellular apoptosis

Confocal microscopy. A549 cells was incubated with different concentration complex **Ir6** at 37 °C in 5% CO_2 for 24 h. After treatment, the cells were stained with AO/EB solution (100 μg mL^{-1} AO, 100 μg mL^{-1} EB). Samples were washed three times with 1× PBS and observed under an confocal microscopy (LSM/880NLO) immediately.

Flow cytometry. Apoptotic populations of the cells was measured by flow cytometry using an Annexin V-FITC apoptosis detection kit (Beyotime Institute of Biotechnology, China) according to the manufacturer's instructions. Briefly, A549 cells cultured in 6-well plates were exposed to different concentration complex **Ir6** for 24 h. The cell suspension was stained with 5 μL Annexin V-FITC and 10 μl of PI at room temperature for 20 min in the dark. The samples were analyzed immediately by flow cytometry (ACEA NovoCyte, Hangzhou, China).

ROS detection

Flow cytometry analysis of ROS generation in the cells caused by exposure to iridium complexes was carried out using the DCFH-DA Flow Cytometry Assay Kit (Beyotime Institute of Biotechnology, China) according to the supplier's instructions. Briefly, After A549 cells being treated with different concentration complex **Ir6** for 6 h or 24 h, for inhibition studies, cells were pre-treated with NAC (10 mM) for 1 h, and then complex **Ir6** were added at different concentrations to against A549 cancer cells. the cells were harvested and collected. Oxidative stress was evaluated with DCFH-DA and flow cytometry according to the manufacturer's instructions. The fluorescence intensity of cells was measured immediately by flow cytometry with excitation at 488 nm and emission at 530 ± 30 nm.

MMP analysis

Confocal microscopy. A549 cells were seeded into 35 mm dishes for confocal microscopy and treated with different concentration complex **Ir6** for 24 h. After the same staining process as described for flow cytometry, the cells were observed under a confocal microscope (LSM/880NLO).

Flow cytometry. MMP was assessed by JC-1 staining. A549 cells incubated 24 h with Ir(III) complexes for various concentration (0.25× IC_{50}, 0.5× IC_{50}, and 1× IC_{50}) were trypsinized and collected, then stained with JC-1 Flow Cytometry Assay Kit (Beyotime Institute of Biotechnology, China) following the manufacture's protocol. The results were obtained by flow cytometry.

AO staining

A549 cells seeded into six-well plate (Corning) were exposed to complex **Ir6** at the indicated concentrations for 12 h. For inhibition studies, cells were pre-treated with NAC (10 mM) for 1 h, and then complex **Ir6** was added at concentrations of 1 × IC_{50} and 2 × IC_{50} against A549 cancer cells. The cells were then washed twice with PBS and incubated with AO (5 μM) at 37 °C for 15 min. The cells were washed twice with PBS and visualized by confocal microscopy (LSM/880NLO). Emission was collected at 510 ± 20 nm (green) and 625 ± 20 nm (red) upon excitation at 488 nm.

Immunofluorescence

Cathepsin B activity was detected using the immunofluorescence according to the manufacturer's instructions. Briefly, A549 cells seeded into six-well plate were exposed to complex **Ir6** at the indicated concentrations for 12 h. For inhibition studies, cells were pre-treated with NAC (10 mM) for 1 h, and then complex **Ir6** was added at concentrations of 1 × IC_{50} and 2 × IC_{50} against A549 cancer cells. A549 cells were fixed with 100% methanol for 15 min at -20˚C and then washed three times with PBS for 5 min per wash. The cells were blocked in blocking buffer for 60 minutes, followed by overnight incubation at 4˚C with primary antibody Cathepsin B XP® Rabbit mAb (Cell Signaling). The following day, cells were washed with PBS three times, followed by 2 h incubation with secondary antibody Anti-Rabbit IgG (H+L) (abcam) at room temperature, and three washes with PBS. Digital images were collected using a confocal microscopy (LSM/880NLO, Germany) immediately. Emission was collected at 650 ± 20 nm upon excitation at 594 nm.

Antimetastatic properties

A549 cells (1,500,000 per well) were seeded in 2000 μL media in 6-well plates and allowed to attach and grow to form a confluent monolayer. Each well of the plates was marked with a horizontal line passing through the center of bottom in advance. Wounds were created perpendicular to the lines by 10 μL tips, and unattached cells were removed by washing with PBS (pH 7.4). Complex **Ir6** in DMEM with 1% FBS was added and cells incubated at 37 ºC under 5% CO_2 for imaging. DMEM with 1% FBS was used to suppress cell proliferation. Images were captured at t = 0 h, 12 h and 24 h at the same position of each well. Experiments were repeated for at least three times.

Colony Formation Assay

A549 cells (3 × 10^2 per well) were plated in 6-well plates. After an overnight incubation, the cells were treated with various concentrations of **Ir6** dissolved in DMSO. Some cells were treated with vehicle (DMSO) only as negative control. After 24 h, the medium was removed, and cells were allowed to grow for 10 days. Then, the cells were fixed with methanol for 15 min and then stained with 0.1% crystal violet for 15 min. After washing away the crystal violet, the plates were photographed, and one colony was defined to be an aggregate of >50 cells. Experiments were repeated for at least three times.

Interaction with CT DNA

DNA binding experiments were carried out in Tris-HCl/KCl buffer (5 mM Tris–HCl/10 mM NaCl buffer solution, pH = 7.2) using DMSO solutions of complex **Ir6**, and then diluting them suitably with buffer to the required concentrations. For every sample, the complexes concentration was constant, a concentrated solution of CT DNA was added (ε_{260}, CT DNA = 6600 M^{-1} cm^{-1} per nucleotide). A reference cell loaded with buffer was necessary, in which the DNA was added each time, to minimize the changes due to the DNA in absorption at 260 nm. After every addition, samples were incubated under physiological conditions (5 mM Tris–HCl/10 mM NaCl buffer solution, pH = 7.2) at room temperature for 10 min equilibration time, and then the UV-visible spectra were recorded. Spectra were collected from 200–600 nm after successive addition of ctDNA (0-0.057 mM) into 3 mL solution of complex (5 μM). The absorbance (A) of the most red-

shifted band of each investigated complex was recorded after successive additions of CT DNA. Interactions of the complex **Ir6** with DNA were fitted to Benesi–Hildebrand equation (Eq. 1)[2] to calculate the binding constants K_b.

$$\frac{[DNA]}{(\varepsilon_a - \varepsilon_f)} = \frac{[DNA]}{(\varepsilon_b - \varepsilon_f)} + \frac{1}{K_b(\varepsilon_b - \varepsilon_f)} \quad (1)$$

where [DNA] is the concentration of DNA and the apparent absorption coefficient, ε_a, corresponds to A_{obs} /[compound]. ε_b and ε_f refer to the extinction coefficient of the complexes in its bound and free form, respectively. The plot of [DNA] / (ε_a-ε_f) versus [DNA] gives a straight line and the binding constants K_b were calculated as slope / intercept ratio.

Gel electrophoresis experiment

Different concentrations of complex **Ir6** and 10 μM DNA were incubated at 310 K for 24 h. Gel electrophoresis experiments were carried out with pBR322 DNA, in 0.8% agarose solution, at 5 V cm^{-1} for 1.5 h using TAE buffer (40 mM Tris, 1 mM EDTA (disodium salt), pH 8.3). The pBR322 DNA was stained with 0.5 mg ml^{-1} GelRed. Gel electrophoresis was performed on a DYY-12C gel electrophoresis spectrometer. Agarose gel electrophoresis of pBR322 DNA was visualized using a gel imaging system (Smart Gel 600, China).

Synthesis of dimer $[Ir(ppz)_2]_2Cl_2$ and ligands imine-N-heterocyclic carbene

The chloro-bridged dinuclear iridium(III) precursor $[Ir(ppz)_2]_2Cl_2$ was synthesized according to previously literature procedure.[3] The ligands imine-N-heterocyclic carbene were prepared according to previously reported.[4]

Synthesis of Ir(III) complexes Ir1-Ir6:

Synthetic procedure of the complexes: A 100 mL Schlenk flask was charged with a mixture of Ligand (0.21 mmol), Ag_2O (0.11 mmol), and $[Ir(ppz)_2]_2Cl_2$ (0.10 mmol) in CH_2Cl_2 (20 mL) were refluxed overnight at 95 °C. After cooling to ambient temperature, KPF_6 (1.26 mmol) was added and the solution was allowed to further stir 30 min. The mixture was filtration through celite to remove excess Ag_2O and washed with CH_2Cl_2. The solvent was removed under reduced pressure and crude product was recrystallized from CH_2Cl_2 and hexane solution to give a colorless solid. ^{1}H NMR of complexes **Ir1-Ir6** are shown in **Figures S7-S12** and mass spectroscopy are shown in **Figure S13**.

Complex Ir1: Yield: 109 mg (72.6%). ^{1}H NMR (500 MHz, DMSO-d_6) δ 8.87 (d, J = 2.9 Hz, 1H), 8.60 (d, J = 2.8 Hz, 1H), 8.20 (d, J = 2.2 Hz, 1H), 8.03 (d, J = 2.2 Hz, 1H), 7.88 (d, J = 2.1 Hz, 1H), 7.59 (d, J = 7.4 Hz, 1H), 7.47 (d, J = 2.2 Hz, 1H), 7.11 (d, J = 7.7 Hz, 1H), 6.86 (t, J = 7.6 Hz, 1H), 6.79 (t, J = 2.6 Hz, 1H), 6.77 – 6.74 (m, 1H), 6.72 (t, J = 6.6 Hz, 2H), 6.66 – 6.58 (m, 3H), 6.53 (t, J = 7.5 Hz, 1H), 6.31 (d, J = 8.0 Hz, 1H), 5.90 (dd, J = 7.6, 0.7 Hz, 1H), 3.13 (s, 3H), 2.57 (s, 3H), 2.18 (s, 3H), 1.18 (s, 3H). ESI-MS (m/z): calcd for $C_{32}H_{31}IrN_7$: 706.2270, found: 706.1502; elemental anallysis calcd (%) for $C_{32}H_{31}F_6IrN_7P$: C, 45.17; H, 3.67; N, 11.52. Found: C, 45.21; H, 3.68; N, 11.49.

Complex Ir2: Yield: 137 mg (81.3%). ^{1}H NMR (500 MHz, DMSO-d_6) δ 8.87 (d, J = 2.9 Hz, 1H), 8.60 (d, J = 2.8 Hz, 1H), 8.23 (d, J = 2.3 Hz, 1H), 8.03 (d, J = 2.2 Hz, 1H), 7.79 (d, J = 2.1 Hz, 1H), 7.62 – 7.52 (m, 2H), 7.11 (d, J = 7.6 Hz, 1H), 6.86 (t, J = 7.6 Hz, 1H), 6.81 (t, J = 2.6 Hz, 1H), 6.75 (dd, J = 5.0, 2.4 Hz, 1H), 6.71 (t, J = 6.4 Hz, 2H), 6.64 – 6.59 (m, J = 8.7, 7.0, 1.5 Hz,

3H), 6.53 (t, *J* = 7.2 Hz, 1H), 6.32 (dd, *J* = 7.3, 1.0 Hz, 1H), 5.88 (dd, *J* = 7.6, 0.9 Hz, 1H), 3.49 (q, *J* = 7.1 Hz, 2H), 2.57 (s, 3H), 2.17 (s, 3H), 1.18 (s, 3H), 0.64 (t, *J* = 7.2 Hz, 3H). ESI-MS (m/z): calcd for $C_{33}H_{33}IrN_7$: 720.2427, found: 720.1749; elemental anallysis calcd (%) for $C_{33}H_{33}F_6IrN_7P$: C, 45.83; H, 3.85; N, 11.34. Found: C, 45.67; H, 3.68; N, 11.49.

Complex Ir3: Yield: 128 mg (87.2%). ^{1}H NMR (500 MHz, DMSO-d_6) δ 8.87 (d, *J* = 2.9 Hz, 1H), 8.61 (d, *J* = 2.8 Hz, 1H), 8.29 (d, *J* = 2.3 Hz, 1H), 8.01 (d, *J* = 2.2 Hz, 1H), 7.79 (d, *J* = 2.1 Hz, 1H), 7.73 (d, *J* = 2.3 Hz, 1H), 7.59 (d, *J* = 7.2 Hz, 1H), 7.11 (d, *J* = 7.6 Hz, 1H), 6.90 – 6.84 (m, 1H), 6.83 – 6.79 (m, 1H), 6.75 (dd, *J* = 5.0, 2.4 Hz, 1H), 6.72 (t, *J* = 6.1 Hz, 2H), 6.63 (td, *J* = 7.7, 1.1 Hz, 2H), 6.60 (dd, *J* = 6.3, 2.4 Hz, 1H), 6.55 – 6.50 (m, 1H), 6.34 (dd, *J* = 7.3, 1.0 Hz, 1H), 5.84 (dd, *J* = 7.6, 0.9 Hz, 1H), 3.95 – 3.85 (m, *J* = 13.5, 6.8 Hz, 1H), 2.57 (s, 3H), 2.17 (s, 3H), 1.26 (d, *J* = 6.8 Hz, 3H), 1.20 (s, 3H), 0.51 (d, *J* = 6.7 Hz, 3H). ESI-MS (m/z): calcd for $C_{34}H_{35}IrN_7$: 734.2583, found: 734.1961; elemental anallysis calcd (%) for $C_{34}H_{35}F_6IrN_7P$: C, 46.46; H, 4.01; N, 11.16. Found: C, 45.57; H, 3.98; N, 11.18.

Complex Ir4: Yield: 123 mg (74.5%). ^{1}H NMR (500 MHz, DMSO-d_6) δ 8.88 (d, *J* = 2.9 Hz, 1H), 8.65 (d, *J* = 2.8 Hz, 1H), 8.09 (d, *J* = 2.2 Hz, 1H), 7.98 (d, *J* = 2.1 Hz, 1H), 7.64 (d, *J* = 2.2 Hz, 1H), 7.55 (d, *J* = 7.2 Hz, 1H), 7.46 (d, *J* = 2.2 Hz, 1H), 7.25 (d, *J* = 7.7 Hz, 1H), 7.02 (t, *J* = 7.6 Hz, 1H), 6.96 (dd, *J* = 7.7, 1.4 Hz, 1H), 6.91 (dd, *J* = 7.5, 1.3 Hz, 1H), 6.87 – 6.79 (m, 3H), 6.69 (td, *J* = 7.8, 1.2 Hz, 1H), 6.59 (dd, *J* = 12.3, 7.6 Hz, 2H), 6.33 (dd, *J* = 7.2, 0.9 Hz, 1H), 5.37 (d, *J* = 8.6 Hz, 1H), 3.41 – 3.35 (m, 1H), 3.11 (s, 3H), 2.66 (s, 3H), 2.00 – 2.08 (m, *J* = 13.2, 6.5 Hz, 1H), 1.14 (d, *J* = 6.7 Hz, 3H), 1.08 (d, *J* = 6.6 Hz, 3H), 0.94 (d, *J* = 6.7 Hz, 3H), 0.23 (d, *J* = 6.6 Hz, 3H). ESI-MS (m/z): calcd for $C_{36}H_{39}IrN_7$: 762.2896, found: 762.2030; elemental anallysis calcd (%) for $C_{36}H_{39}F_6IrN_7P$: C, 47.68; H, 4.33; N, 10.81. Found: C, 47.88; H, 4.34; N, 10.99. Crystals of suitable for X-ray diffraction analysis were obtained by slow diffusion ether into a concentrated solution of the complex **Ir4** in CH_2Cl_2 at room temperature.

Complex Ir5: Yield: 142 mg (89.7%). ^{1}H NMR (500 MHz, DMSO-d_6) δ 8.88 (d, *J* = 2.9 Hz, 1H), 8.65 (d, *J* = 2.8 Hz, 1H), 8.12 (d, *J* = 2.2 Hz, 1H), 7.90 (d, *J* = 2.1 Hz, 1H), 7.65 (d, *J* = 2.1 Hz, 1H), 7.58 (d, *J* = 2.2 Hz, 1H), 7.54 (d, *J* = 7.7 Hz, 1H), 7.25 (d, *J* = 7.8 Hz, 1H), 7.01 (t, *J* = 7.6 Hz, 1H), 6.96 (d, *J* = 6.6 Hz, 1H), 6.91 (d, *J* = 7.4 Hz, 1H), 6.84 (ddd, *J* = 6.9, 5.2, 2.5 Hz, 3H), 6.68 (t, *J* = 7.6 Hz, 1H), 6.59 (dd, *J* = 13.5, 6.7 Hz, 2H), 6.35 (d, *J* = 6.7 Hz, 1H), 5.35 (d, *J* = 7.7 Hz, 1H), 3.35 – 3.52 (m, *J* = 13.1, 6.7 Hz, 2H), 3.26 – 3.21 (m, 1H), 2.66 (s, 3H), 2.05 (dt, *J* = 13.1, 6.4 Hz, 1H), 1.13 (d, *J* = 6.7 Hz, 3H), 1.09 (d, *J* = 6.6 Hz, 3H), 0.94 (d, *J* = 6.6 Hz, 3H), 0.61 (t, *J* = 7.2 Hz, 3H), 0.23 (d, *J* = 6.6 Hz, 3H). ESI-MS (m/z): calcd for $C_{37}H_{41}IrN_7$: 776.3053, found: 776.2526; elemental anallysis calcd (%) for $C_{37}H_{41}F_6IrN_7P$: C, 48.25; H, 4.49; N, 10.65. Found: C, 48.28; H, 4.51; N, 10.49.

Complex Ir6: Yield: 128 mg (84.3%). ^{1}H NMR (500 MHz, DMSO-d_6) δ 8.88 (d, *J* = 2.9 Hz, 1H), 8.65 (d, *J* = 2.8 Hz, 1H), 8.17 (d, *J* = 2.3 Hz, 1H), 7.90 (d, *J* = 2.1 Hz, 1H), 7.74 (d, *J* = 2.3 Hz, 1H), 7.62 (d, *J* = 2.1 Hz, 1H), 7.54 (d, *J* = 7.9 Hz, 1H), 7.25 (d, *J* = 7.8 Hz, 1H), 7.01 (t, *J* = 7.6 Hz, 1H), 6.98 – 6.94 (m, 1H), 6.90 (d, *J* = 7.5 Hz, 1H), 6.84 (ddd, *J* = 10.5, 5.1, 2.6 Hz, 3H), 6.69 (t, *J* = 7.6 Hz, 1H), 6.59 (q, *J* = 7.3 Hz, 2H), 6.37 (d, *J* = 7.2 Hz, 1H), 5.31 (d, *J* = 7.6 Hz, 1H), 3.94 – 3.83 (m, 1H), 3.47 – 3.39 (m, 1H), 2.66 (s, 3H), 2.13 – 2.04 (m, 1H), 1.26 (d, *J* = 6.8 Hz, 3H), 1.11 (dd, *J* = 13.2, 6.7 Hz, 6H), 0.94 (d, *J* = 6.6 Hz, 3H), 0.46 (d, *J* = 6.7 Hz, 3H), 0.24 (d, *J* = 6.6 Hz, 3H). ESI-MS (m/z): calcd for $C_{38}H_{43}IrN_7$: 790.3209, found: 790.2943; elemental anallysis calcd (%) for $C_{38}H_{43}F_6IrN_7P$: C, 48.81; H, 4.64; N, 10.49. Found: C, 48.59; H, 4.62; N, 10.49.

Reference

1. H. Huang, P. Zhang, B. Yu, Y. Chen, J. Wang, L. Ji and H. Chao, *J. Med. Chem.*, 2014, **57**, 8971-8983.
2. M. Mohamadi, A. Hassankhani, S. Y. Ebrahimipour and M. Torkzadeh-Mahani, *Int. J. Biol. Macromol.*, 2017, **94**, 85-95.
3. D. L. Davies, M. P. Lowe, K. S. Ryder, K. Singh and S. Singh, *Dalton Trans.*, 2011, **40**, 1028-1030.
4. Y. Yang, L. Guo, Z. Tian, X. Liu, Y. Gong, H. Zheng, X. Ge and Z. Liu, *Chem. Asian J.*, 2018, **13**, 2923-2933.

Table S1. Crystallographic data and structure refinement for complex **Ir4.**

Identification code	**Ir4**
Formula	$C_{36}H_{39}F_6IrN_7P$
MW	906.91
Cryst	yellow block
Cryst size (mm)	0.32×0.23×0.20
λ (Å)	0.71073
Temp. (K)	298(2)
Cryst syst.	Orthorhombic
Space group	Pbca
a (Å)	15.6458(13)
b (Å)	19.5934(17)
c (Å)	23.431(2)
α (°)	90
β (°)	90
γ (°)	90
Vol. ($Å^3$)	7182.8(11)
Z	8
density(calc)($Mg·m^{-3}$)	1.677
abs coeff (mm^{-1})	3.831
F(000)	3600
θ range (deg)	2.25 to 25.02
index ranges	-18<=h<=16,-23<=k<=20, -25<=l<=27
reflns collected	28459
indep reflns	6279 [R(int) = 0.0548]
data/restraints/params	6279 / 0 / 503
final R indices	R1 = 0.0329
[I > 2σ(I)]	wR2 = 0.0628
R indices (all data)	R1 = 0.0739, wR2 = 0.0726
GOF	1.098
largest diff. peak and hole (e $Å^{-3}$)	1.144 and -0.667

Table S2. Select bond lengths (Å) and angles (°) for complex **Ir4**.

bond/angle	Ir4
Ir1-N3	2.218(5)
Ir1-N5	2.026(5)
Ir1-N7	2.033(4)
Ir1-C1	2.054(5)
Ir1-C23	2.064(5)
Ir1-C32	2.017(6)
C1-Ir1-N3	76.1(2)
C1-Ir1-C32	98.2(2)
C1-Ir1-N7	83.72(19)
C1-Ir1-N5	102.2(2)
C1-Ir1-C23	175.9(2)
N3-Ir1-C32	173.83(19)
N3-Ir1-N7	97.01(18)
N3-Ir1-C23	100.04(19)
N3-Ir1-N5	91.86(18)
C32-Ir1-N7	79.9(2)
C32-Ir1-C23	85.6(2)
C32-Ir1-N5	91.7(2)
N7-Ir1-C23	95.5(2)
N7-Ir1-N5	170.35(19)
C23-Ir1-N5	79.1(2)

Table S3. In vitro cytotoxicity of the tested complexes **Ir1**−**Ir6** towards different normal cell lines after 24 h incubation.

	IC_{50} (μM)	
Complexes	**BEAS-2B**	**16HBE**
Ir1	7.5 ± 0.3	11.3 ± 0.9
Ir2	6.2 ± 0.1	7.7 ± 0.1
Ir3	5.4 ± 0.7	5.7 ± 0.7
Ir4	2.2 ± 0.1	5.0 ± 1.2
Ir5	2.1 ± 0.5	3.5 ± 0.2
Ir6	1.8 ± 0.4	2.9 ± 0.5
Cisplatin	42.0 ± 2.3	18.6 ± 2.0

Table S4. Iridium amounts in the cytosol, nucleus, membrane and cytoskeleton fractions (fg Ir/ cell) in A549 cells after 1 h of exposure to complex **Ir6** (10 μM).

	Ir fg / cell				
	cytosol	**nucleus**	**membrane**	**cytoskeleton**	**total**
A549	49.23±13.45	18.12±9.72	63.26±24.23	5.05±4.92	141.2±25.45

Table S5. Iridium amounts of A549 cells after 15 min incubation with **Ir6** (10 μM) under different conditions.

	Ir fg / cell			
	37 °C	**CCCP**	**chloroquine**	**4 °C**
A549	118.15±9.37	52.74±5.12	97.33±8.97	11.11±1.62

Table S6. Flow cytometry analysis to determine the percentages of apoptotic cells, using Annexin V-FITC vs PI staining, after exposing A549 cells to complex **Ir6**.

		Population (%)			
Complex	**Ir concentration**	**Viable**	**Early apoptosis**	**Late apoptosis**	**Non-viable**
control		93.99±0.21	0.34±0.01	5.02±0.11	0.66±0.09
Ir6	0.5 × IC_{50}	93.19±0.25	1.61±0.12	5.08±0.13	0.11±0.01
	1 × IC_{50}	75.45±0.39	5.26±0.04	19.08±0.28	0.44±0.15
	2 × IC_{50}	61.78±0.04	18.98±0.20	19.11±0.18	0.13±0.01
	3 × IC_{50}	31.44±0.81	29.79±0.58	38.68±0.23	0.10±0.01

Table S7. The mitochondrial membrane polarization of A549 cells induced by complex **Ir6**.

		Population (%)	
Complex	**Ir concentration**	**JC-1 Aggregates**	**JC-1 Monomers**
Ir6	0.25 × IC_{50}	68.17±3.56	31.83±3.56
	0.5 × IC_{50}	60.75±0.71	39.26±0.71
	1 × IC_{50}	31.20±5.42	68.81±5.42
Negative Control		95.30±0.15	4.71±0.15
Positive Control		21.93±2.32	78.07±2.32

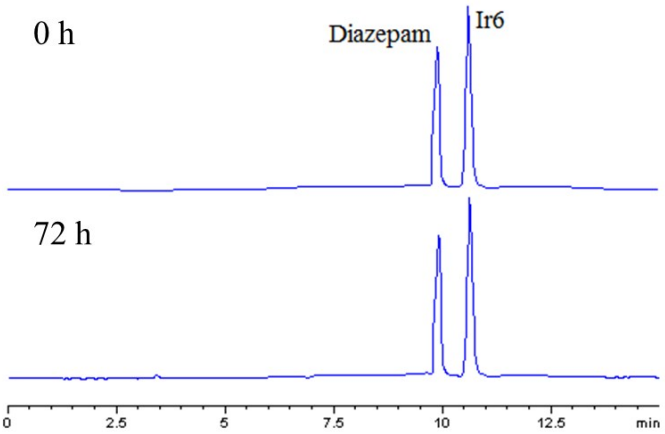

Figure S1. HPLC-UV trace of plasma incubated with complex **Ir6** (10 μM) at t = 0 and 72 h (Diazepam was used as internal standard).

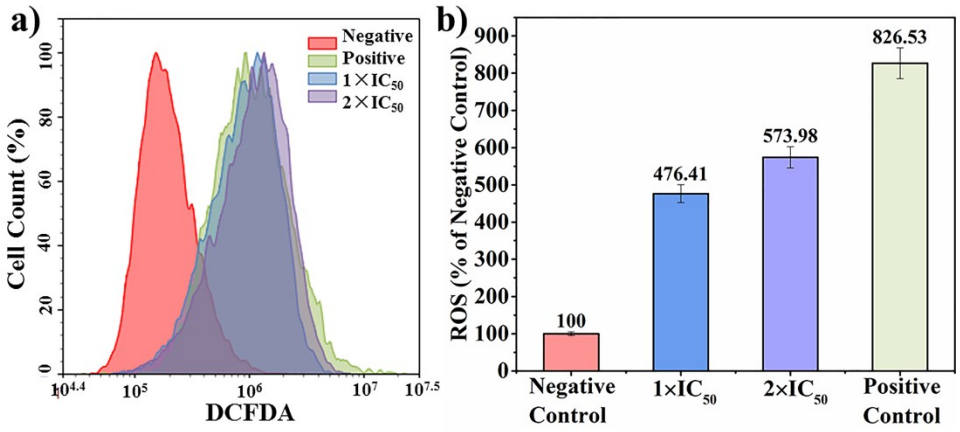

Figure S2. Induction of ROS levels in A549 cells by complex **Ir6** (concentrations used: 1× and 2× IC_{50}) after 24 h at 310 K. a) ROS levels analysis examined by flow cytometry. b) Bar chart showing cell populations ROS levels.

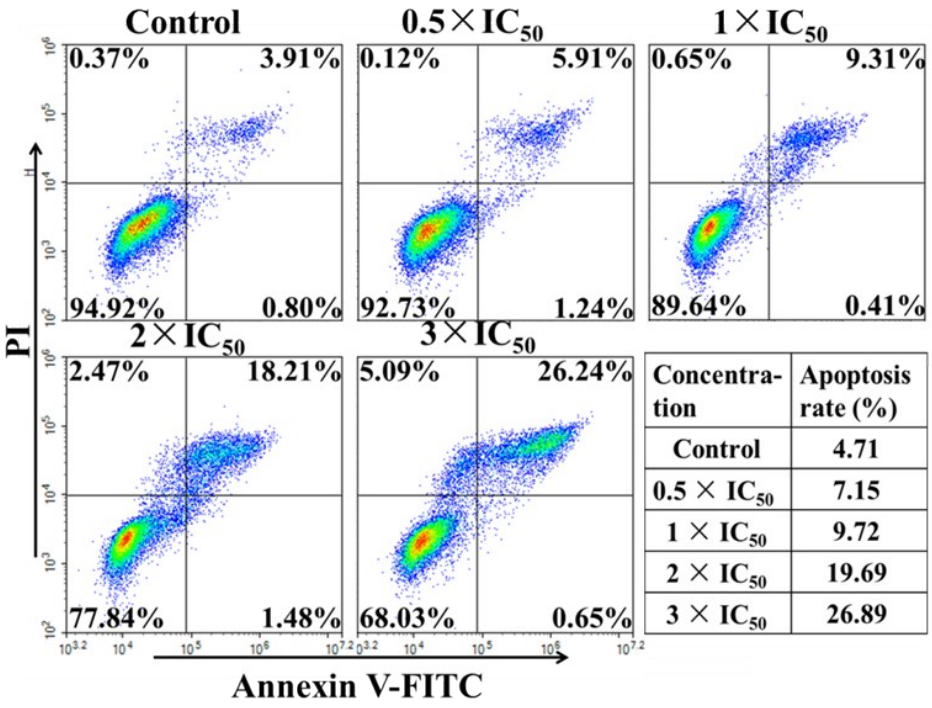

Concentration	Apoptosis rate (%)
Control	4.71
0.5 × IC_{50}	7.15
1 × IC_{50}	9.72
2 × IC_{50}	19.69
3 × IC_{50}	26.89

Figure S3. A549 cells treated with complex **Ir6** in the absence of NAC (10 mM), apoptotic cell examined by flow cytometry.

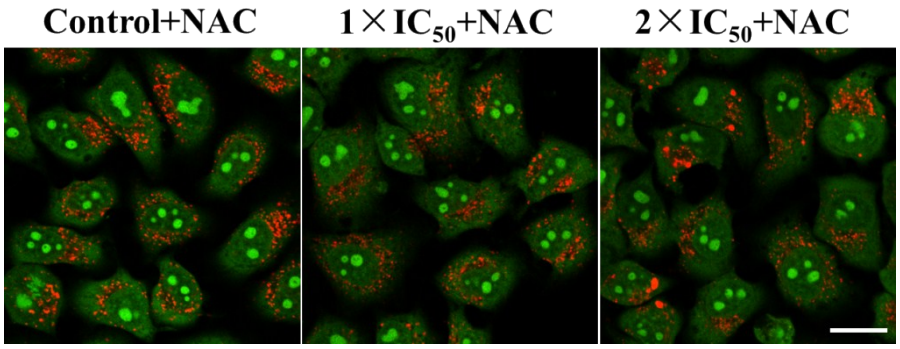

Figure S4. A549 cells were pre-treated with NAC (10 mM) for 1 h. Observation of lysosomal disruption in A549 cells caused by complex **Ir6** with AO (5 μM) staining. Scale bars: 20 μm.

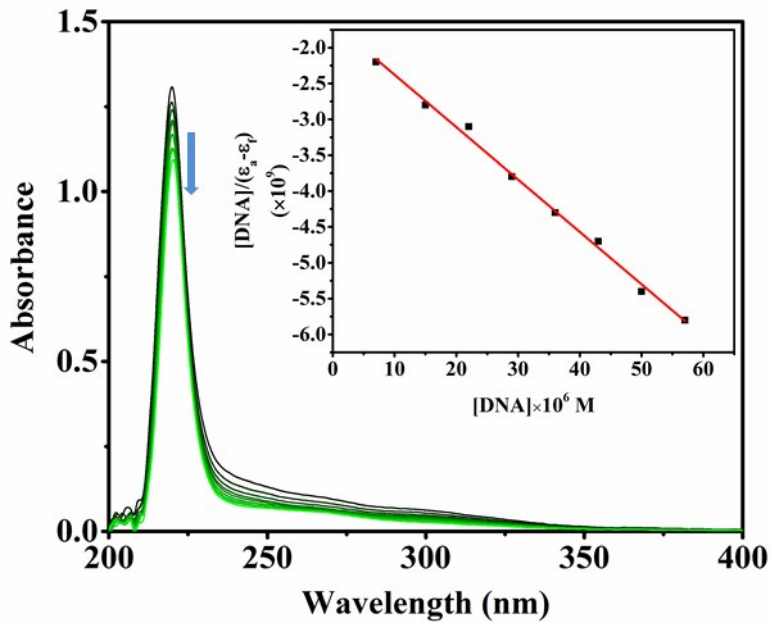

Figure S5. UV-Vis spectrum of complex **Ir6** (5 μM) with an increasing concentration of CT DNA (0-0.057 mM) in 5 mM Tris–HCl/10 mM NaCl buffer solution (pH = 7.2) at room temperature. The arrows show the direction of changes in absorbance upon increasing the concentration of the complex. Inset: Plot of [DNA] / (ε_a-ε_f) vs. [DNA].

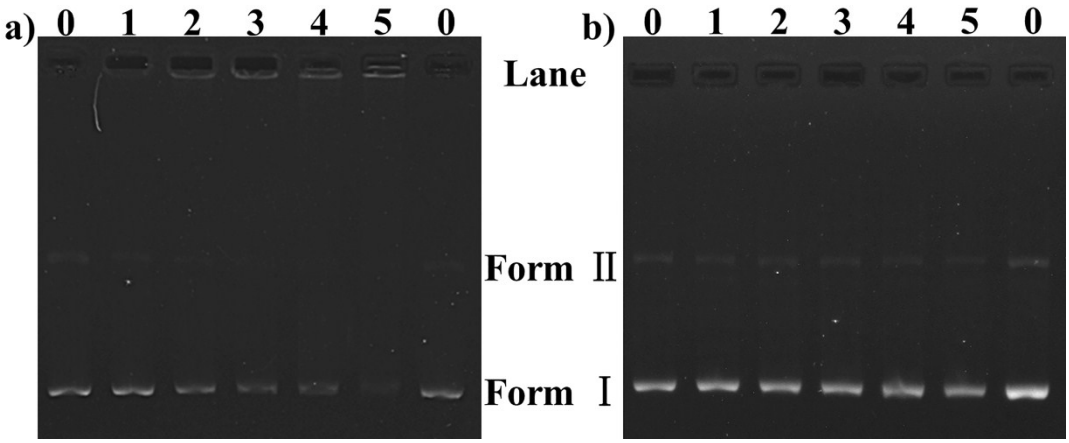

Figure S6. Agarose gel electrophoresis patterns of interaction of pBR322 DNA with various concentrations of complex **Ir6**. Lane 0: DNA control; Lane 1: DNA + 20 μM **Ir6**; Lane 2: DNA + 40 μM **Ir6**; Lane 3: DNA + 60 μM **Ir6**; Lane 4: DNA + 80 μM **Ir6**; Lane 5: DNA +100 μM **Ir6**. a) Complex **Ir6** and DNA incubation for 24 h. b) Complex **Ir6** and DNA incubation for 0 h.

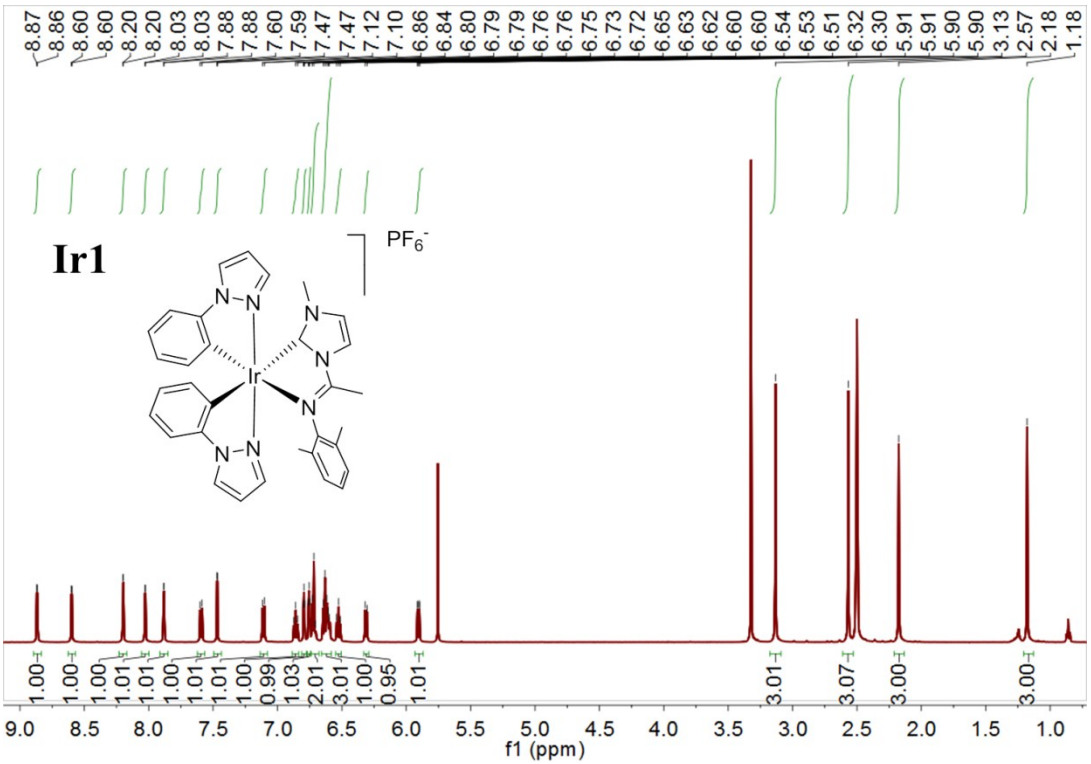

Figure S7. [1]H NMR spectrum of complex **Ir1.**

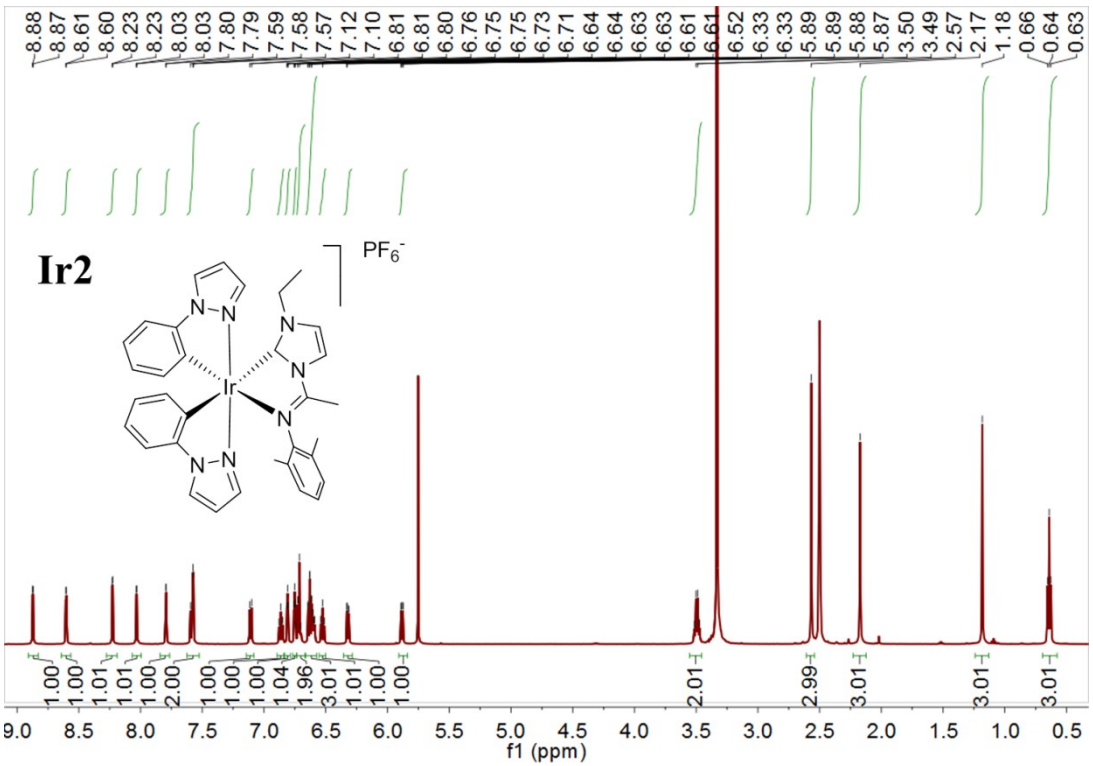

Figure S8. [1]H NMR spectrum of complex **Ir2.**

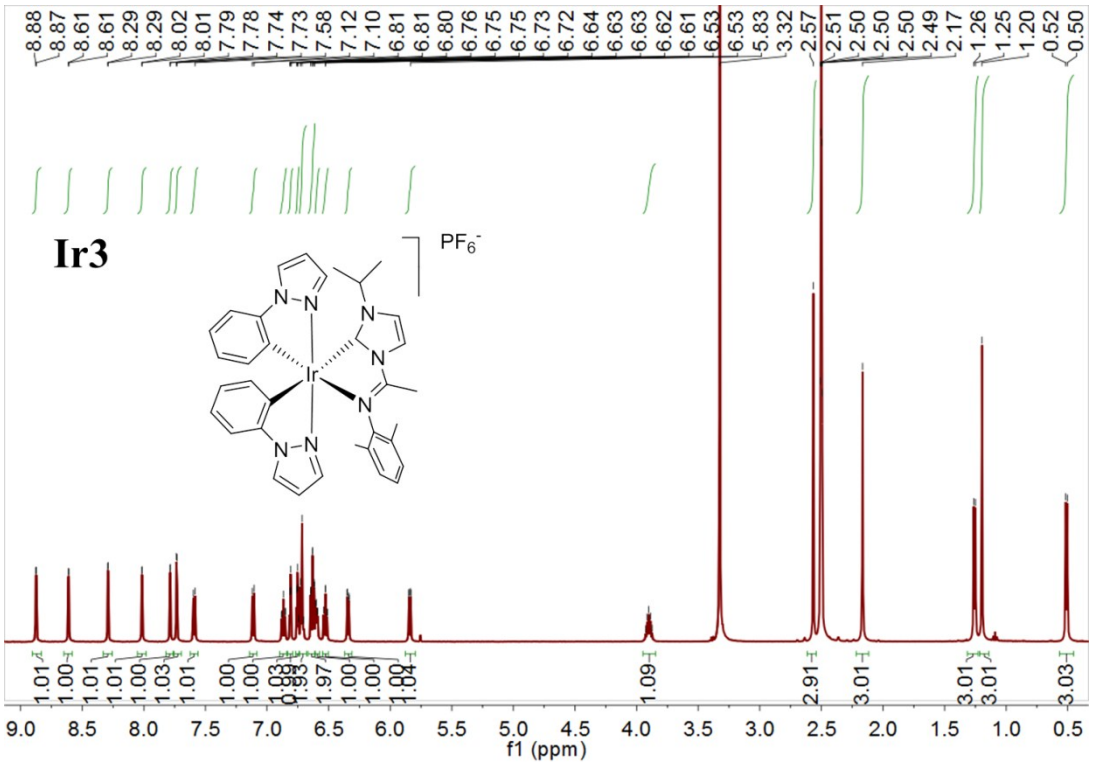

Figure S9. [1]H NMR spectrum of complex **Ir3.**

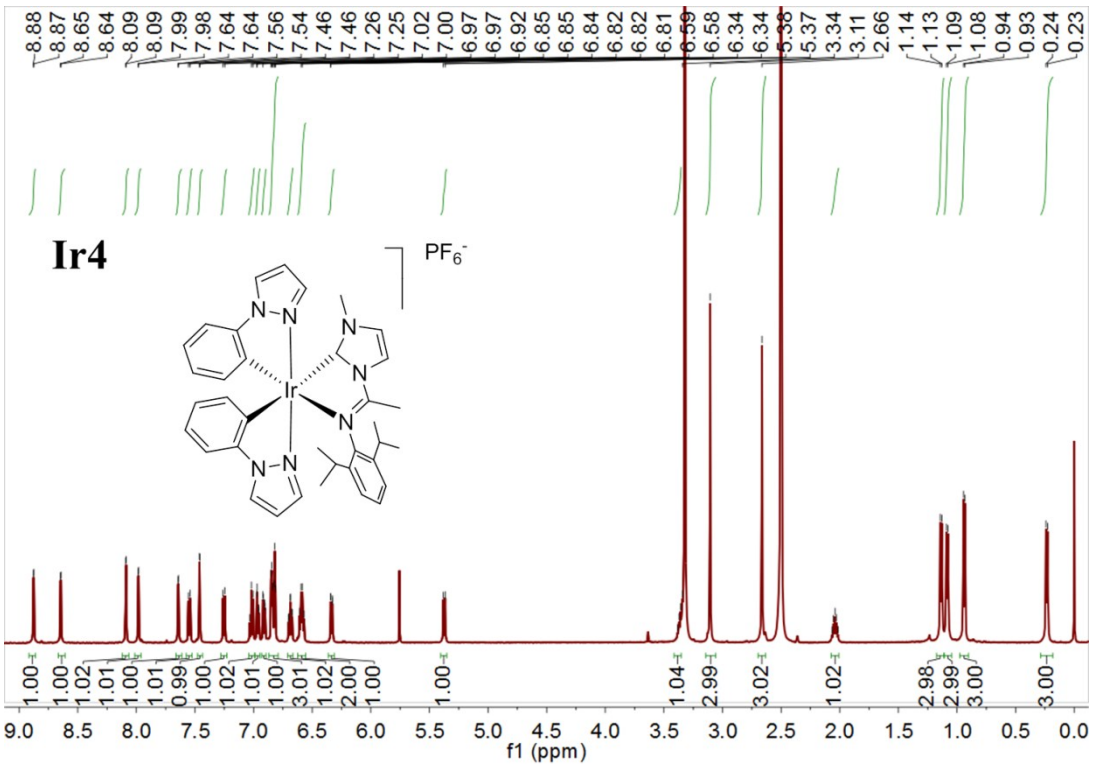

Figure S10. [1]H NMR spectrum of complex **Ir4.**

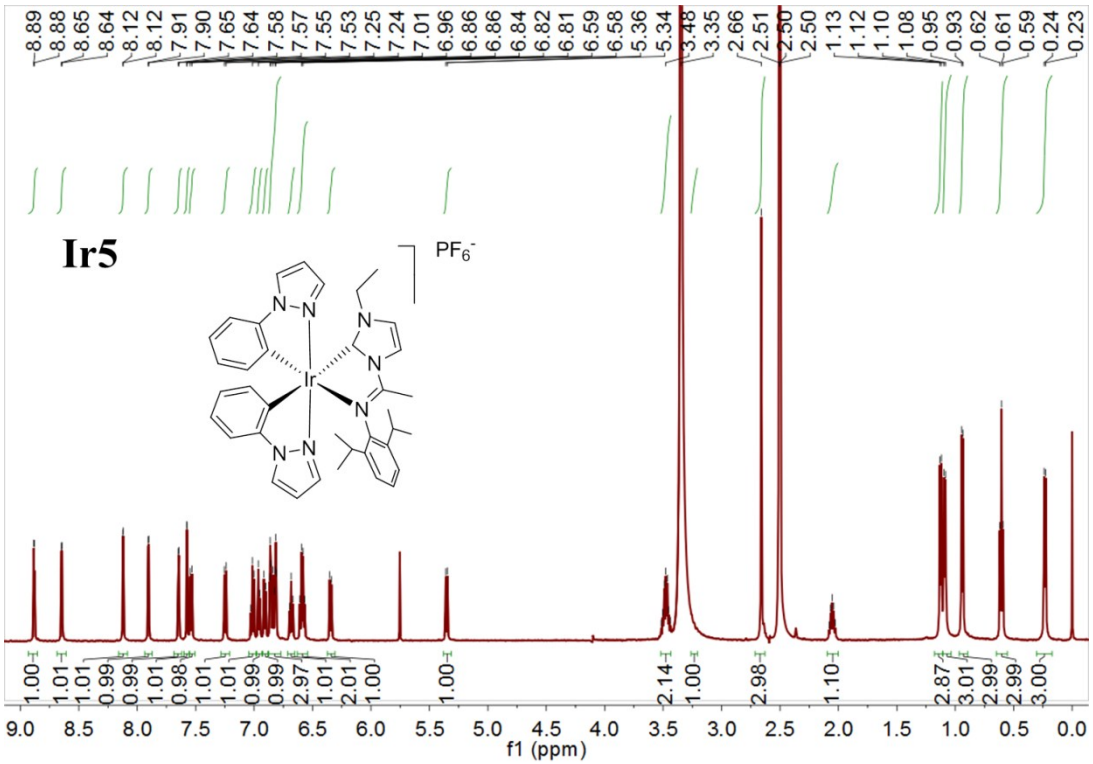

Figure S11. ^{1}H NMR spectrum of complex **Ir5.**

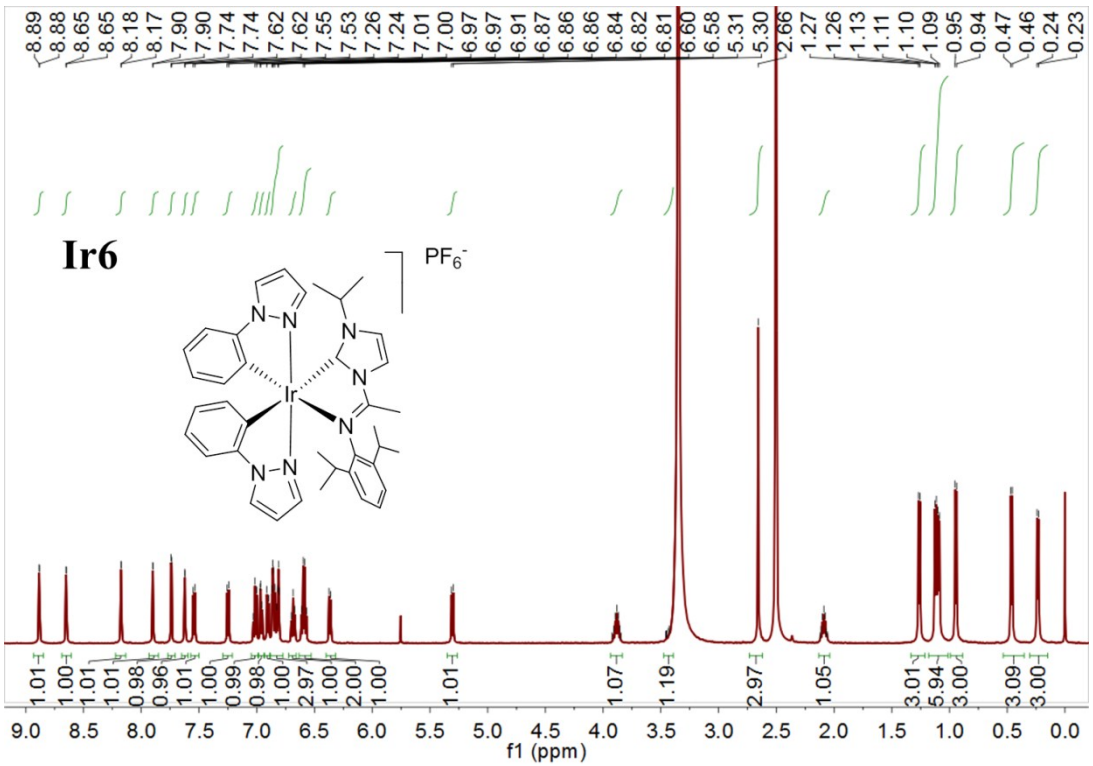

Figure S12. ^{1}H NMR spectrum of complex **Ir6.**

Complex **Ir1.**

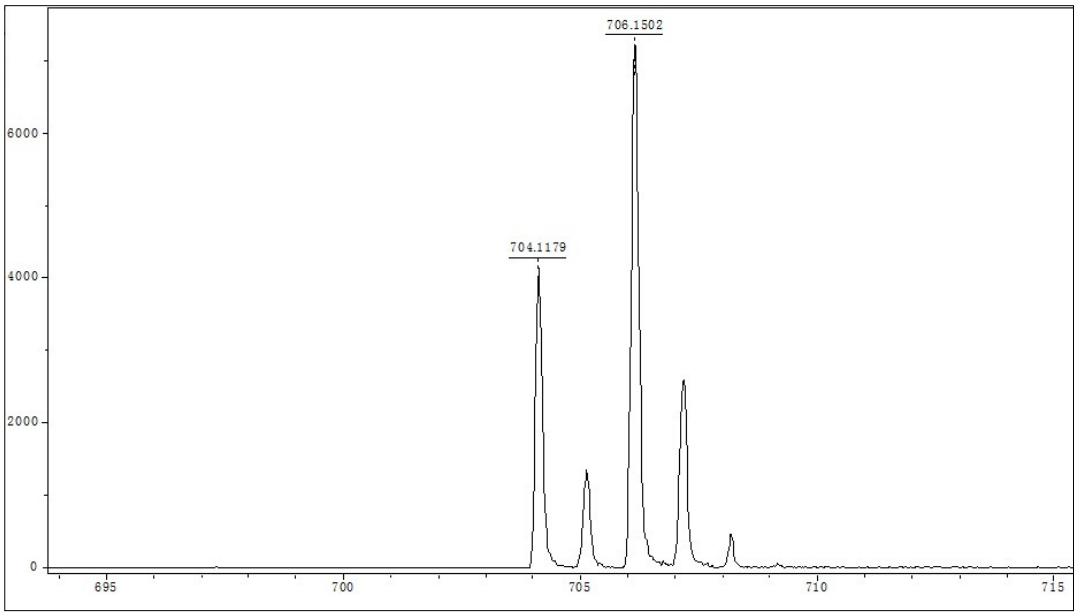

Complex **Ir2.**

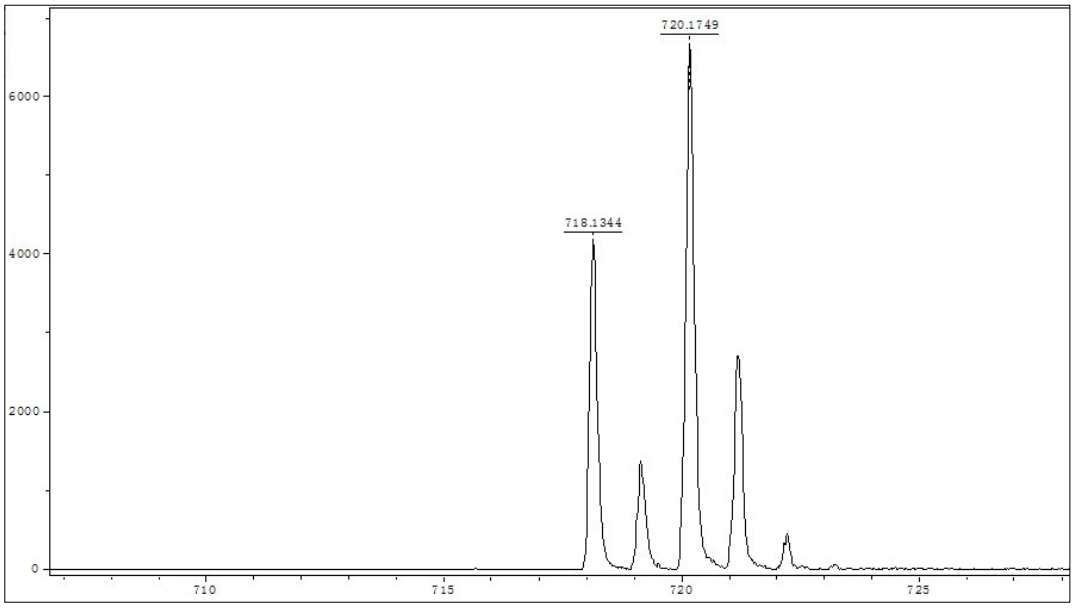

Complex **Ir3.**

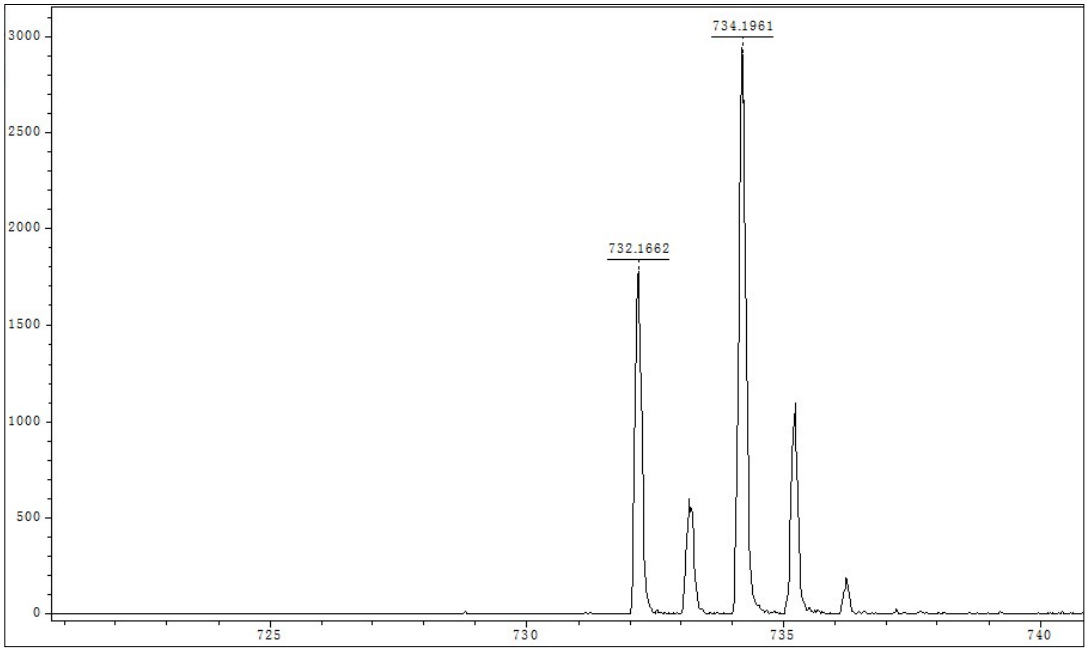

Complex **Ir4.**

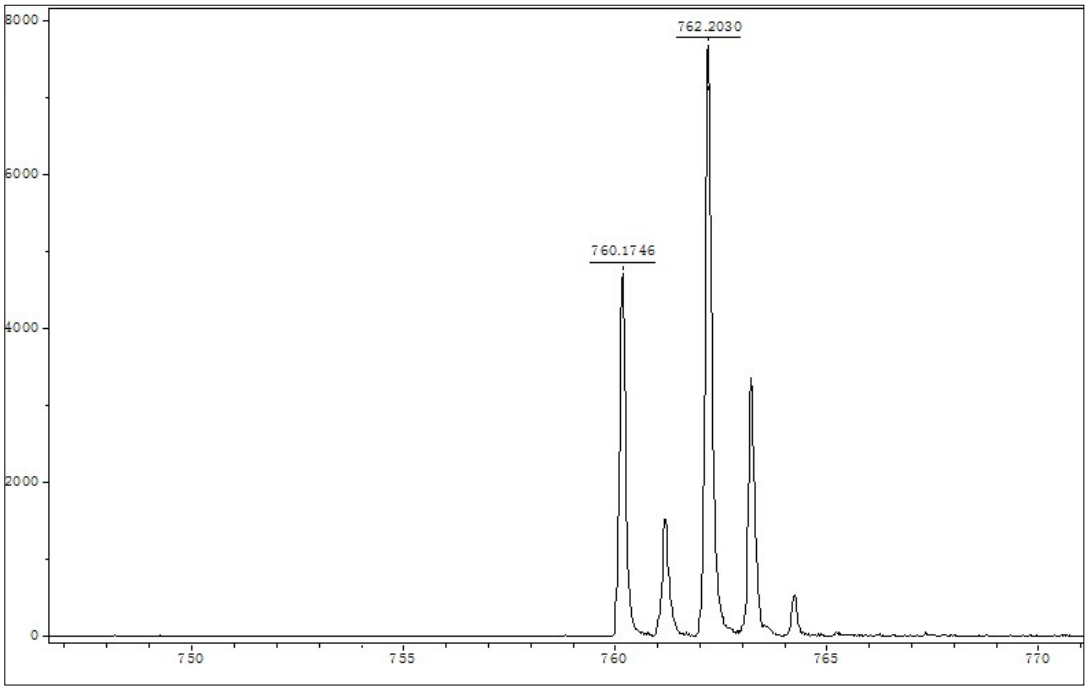

Complex **Ir5.**

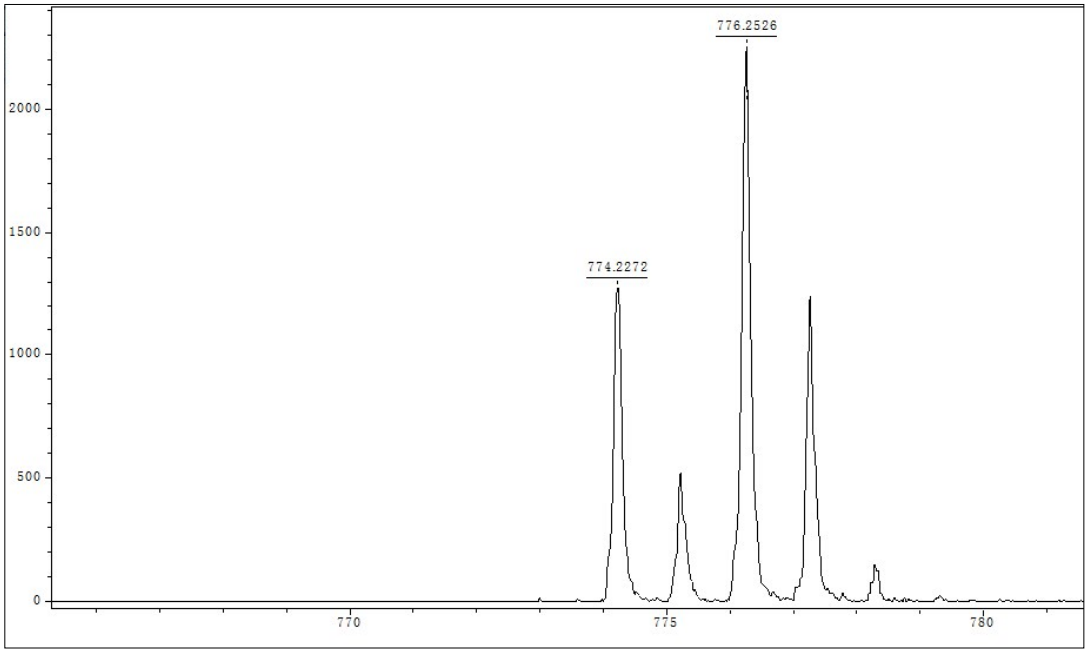

Complex **Ir6.**

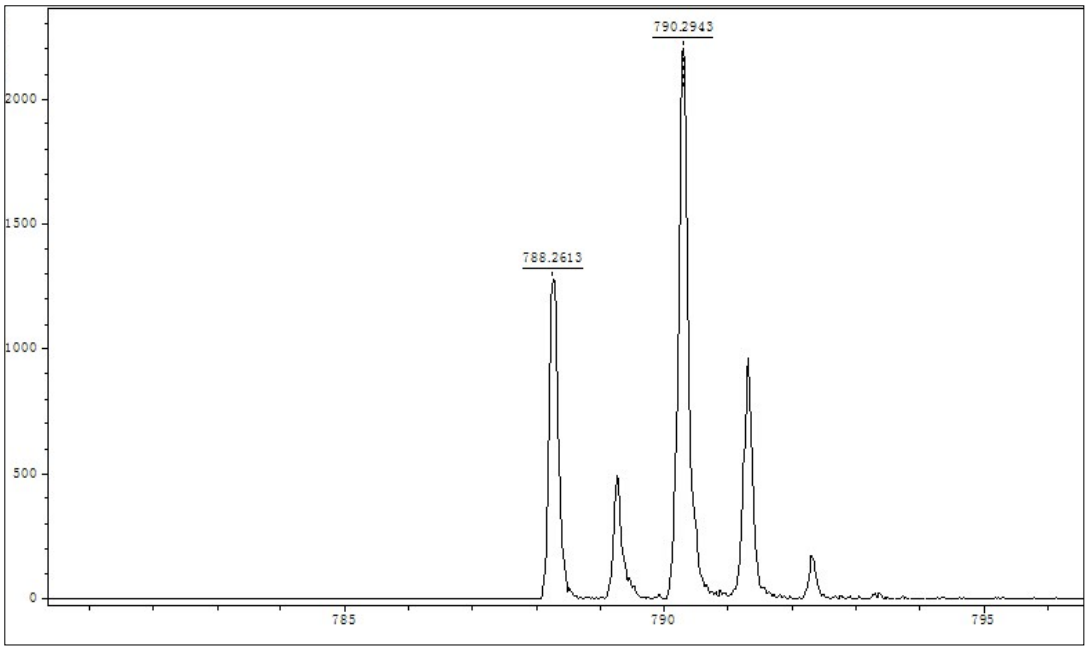

Figure S13. The Mass spectrometry of complexes **Ir1-Ir6**.